

EUROPEAN ORGANIZATION FOR NUCLEAR RESEARCH
CERN — AB DEPARTMENT

CERN-AB-Note-2006-035 ATB
EURISOL-DS/TASK2/TN-05-03

EURISOL-DS Multi-MW Target Neutronic Calculations for the Baseline Configuration of the Multi-MW Target

Adonai Herrera-Martínez, Yacine Kadi

AB Dept. ATB/EET

European Organization for Nuclear Research (CERN)
CH-1211 Geneva 23, Switzerland

Abstract

This document summarises the study performed within the Task #2 of the European Isotope Separation On-Line Radioactive Ion Beam Facility Design Study (EURISOL DS) [1] to design the Multi-MW proton-to-neutron converter.

A preliminary study [2] was carried out in order to understand the nature of the interactions taking place in the proton-to-neutron converter and their impact on the design of the facility. Namely, the target dimensions and material composition, type of incident particle, its energy and the beam profile were analysed in the aforementioned technical note, and their optimum values were suggested in the conclusions.

The present work is based on the results of the previous study and uses the same methodology, namely Monte Carlo simulations with FLUKA [3]. This note describes the performance of a Hg target design and addresses more detailed issues, such as the composition of the fission target and use of a neutron reflector. It also attempts to integrate those components together and estimate the whole performance in terms of number of fissions, isotopic yields and power densities.

The results of these calculations show the feasibility of this Multi-MW target design and the possibility of achieving the aimed fission rates with a reduced fission target. The assembly has been characterised in terms of neutronics and power densities, both key factors in the technical design, due to the high isotopic yields aimed and the large power densities foreseen.

Geneva, Switzerland
30 January, 2006

Table of Contents

PROPOSED BASELINE CONFIGURATION	3
HIGH DENSITY FISSION TARGET.....	9
Natural Uranium Carbide (UnatC).....	9
Depleted Uranium Carbide (²³⁸ UC).....	10
USE OF A NEUTRON REFLECTOR.....	12
2 GEV PROTON BEAM	14
Extended Target Length.....	14
2 GeV Protons on a Short Target.....	16
INTEGRATION OF THE ASSEMBLY	18
CONCLUSIONS.....	19
ACKNOWLEDGEMENTS	20
REFERENCES	20

Proposed Baseline Configuration

Following the results from [2], a baseline configuration was defined. In order to maximise the neutron production, a 15 cm radius 45 cm long Hg proton-to-neutron converter was suggested, surrounded by the fission target and, possibly, by a neutron reflector. Figure 1 shows a schematic view of this preliminary configuration, with a 5 cm gap between the Hg container and the 3 cm thick UC₃ target. An artistic view is also included, showing the assembly in 3D.

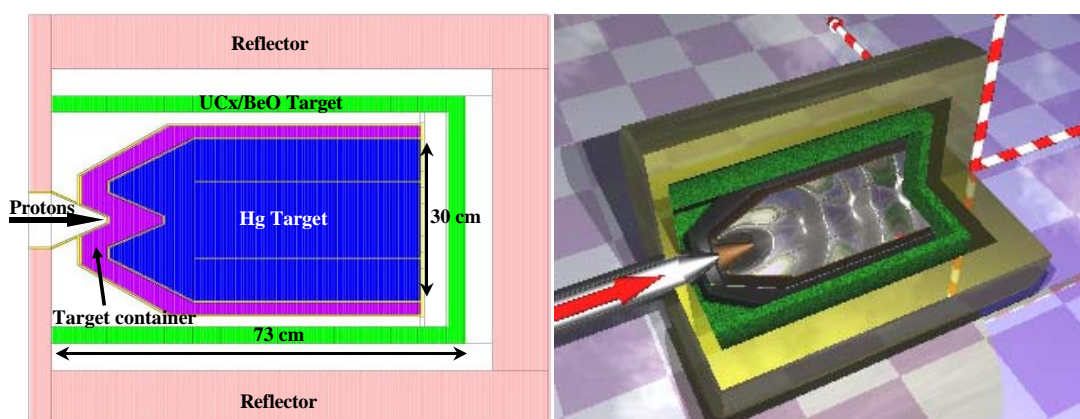


Figure 1. Schematic and artistic views of the baseline configuration, where several components of the facility have been integrated.

In this preliminary configuration, the fission target surrounds the Hg in order to assess the best placement of the final, smaller, fission targets. The use of BeO reflector is suggested to improve the neutron economy and increase the fission densities. A double hull is proposed to ensure the Hg confinement in case of failure in the Hg container, and also to allow the flow of He to cool the beam windows. This “cold window” approach is suggested since, generally, the beam window is the first element to fail in the system. The conical beam-target interface serves two purposes, minimise backscattered particles and distribute the beam heat load in the window along a larger surface.

For the standard set up, the density of the UnatC₃ fission target used was 3 g/cm³, to properly simulate this low-density porous carbide. The 10 cm thick reflector was BeO given the high albedo of this material. A 1 GeV 15 mm σ proton beam was taken due to the good trade between beam size, primary particle containment, target dimensions and power densities.

The containment of these high-energy charged particles has a two-fold relevance: in terms of reducing the number of isobars (generally proton-rich isotopes) produced by protons, which compete during extraction with the fission products (neutron-rich);

and in terms of radioprotection, since primary escapes displace the neutron source outside the assembly, complicating the radiation containment.

This proposed baseline configuration successfully contains most of the primary proton beam inside the Hg target, with only few escapes reaching the fission target and fewer (below 2×10^8 primary/cm²/s/MW of beam) exiting the assembly, as illustrated by Figure 2. These primary particles also present low kinetic energies, due to the ionisation losses undergone through the Hg (distance travelled close to the particle range).

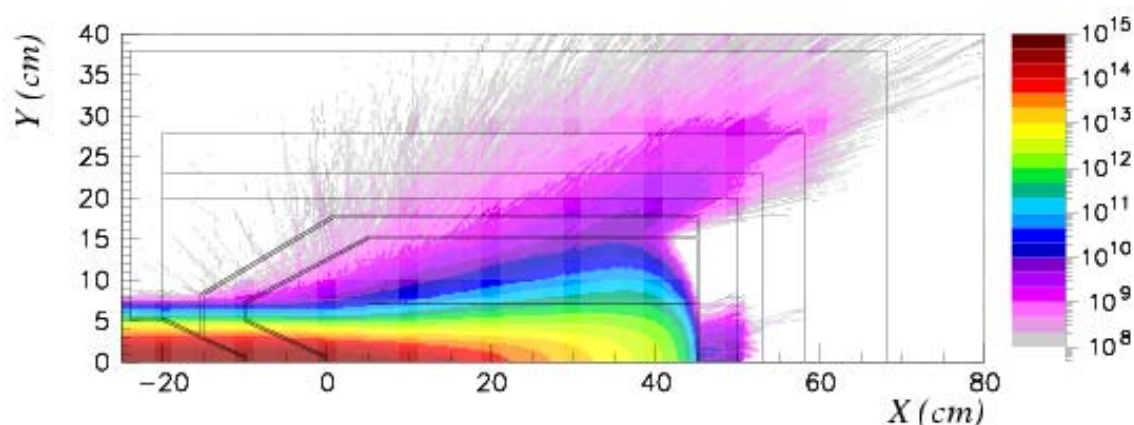


Figure 2. Primary proton flux distribution (primary/cm²/s/MW of beam) for the baseline configuration and a 1 GeV proton beam.

The neutron flux distribution becomes isotropic a few cm away from its centre (~ 10 cm from the impact point, Figure 3). The flux reaching the fission target is $\sim 10^{14}$ n/cm²/s/MW of beam radially, and slightly lower if the fission target is placed in the beam direction at the end of the Hg target (hereby, end cap position). These neutron fluxes, similar to those obtained in conventional nuclear reactors, seem sufficient to produce the aimed $\sim 10^{15}$ fissions per second [4], as will be elaborated later.

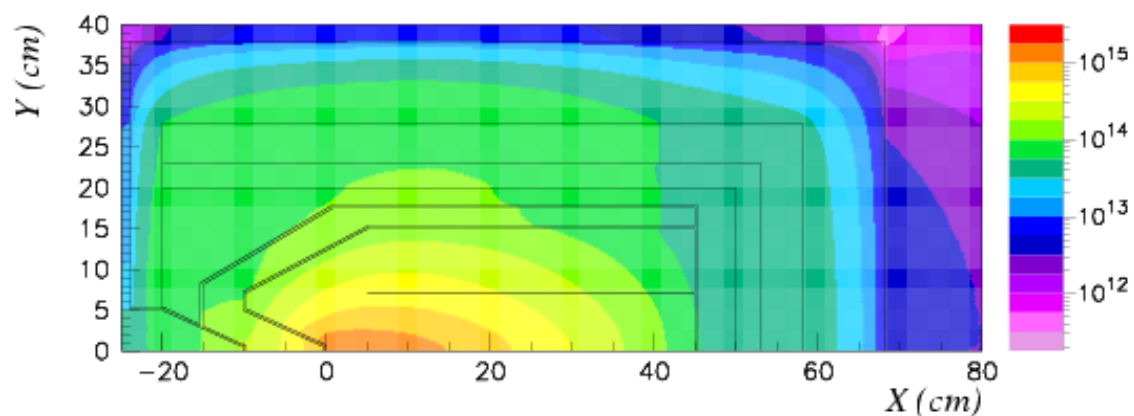


Figure 3. Neutron flux distribution (neutrons/cm²/s/MW of beam) for the baseline configuration and a 1 GeV proton beam.

The neutron energy spectra exiting radially and axially are presented in Figure 4, where the evaporation neutron peak (at ~ 400 keV due to down-scattering ~ 2 MeV) and a high-energy peak (50 MeV radially and 200 MeV axially, from nucleon-nucleon interactions) may be seen. There is a clear advantage in placing the fission targets around the proton-to-neutron converter since the neutron spectrum is higher for most energies, particularly between 1 and 50 MeV, where fissions occur in ^{238}U . Moreover, very high-energy hadrons, coming from forward-peaked direct high-energy nucleon-nucleon interactions, are avoided in the fission target with the radial configuration.

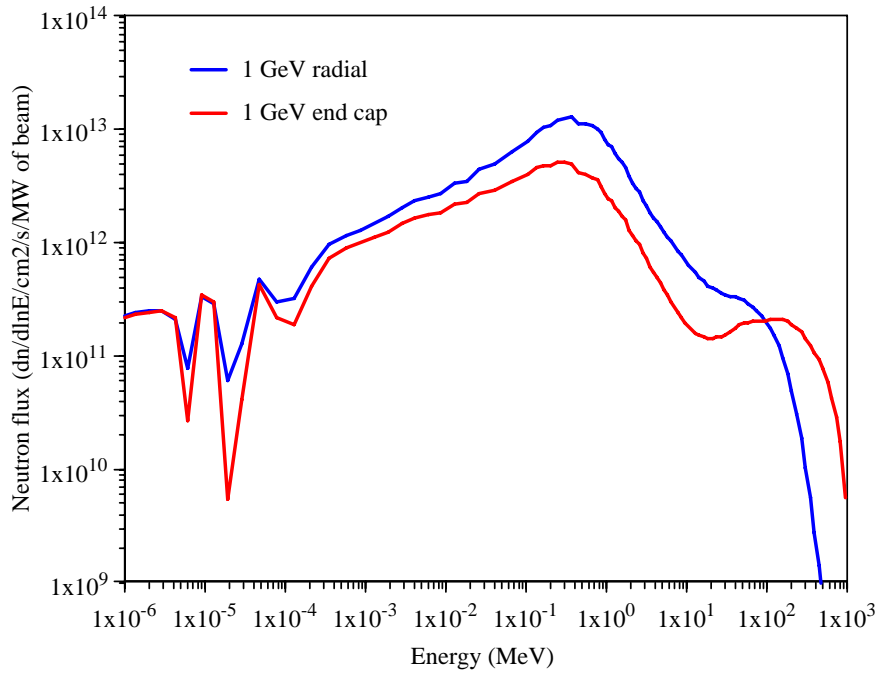


Figure 4. Neutron energy spectra ($\text{dn}/\text{dlnE}/\text{cm}^2/\text{s}/\text{MW}$ of beam) exiting the proton-to-neutron converter radially (blue curve) and axially (red curve).

In terms of neutron balance density, the radius and length of the Hg target could still be reduced by a few cm, given the neutron-absorbing region in the periphery of the converter (indicated by the existence of a neutral balance boundary, Figure 5). This decrease from the dimensions suggested in [2] is due to the effect of the BeO, which reflects back the escaping neutrons. Some of these neutrons are later captured in the periphery of the Hg converter, hence the decrease in the neutron balance.

The neutron production in the Hg target is relatively concentrated, since 70% of the neutrons are generated in a 5 cm radius 20 cm long cylinder (5% of the Hg volume), downstream from the interaction point. Nevertheless, in order to take advantage of the full proton beam and, as elaborated previously, to contain the primary shower, the larger Hg volume is necessary.

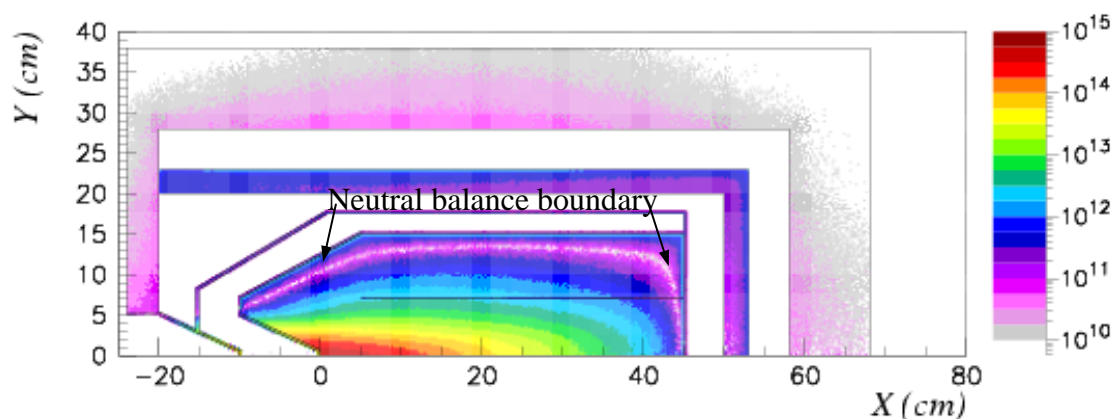


Figure 5. Neutron balance density (sum of the outgoing neutrons minus the incoming ones per cm^3 , for every bin region) in the Multi-MW target assembly.

Fission density is arguably the most relevant single parameter for the design of the Multi-MW target. For this particular set up, the fission density is rather homogeneous ($\sim 10^{11}$ fissions/ $\text{cm}^3/\text{s}/\text{MW}$ of beam, Figure 6). This is particularly positive to enhance ion extraction and to avoid thermal stresses due to temperature differences. Moreover, with this fission density, the aimed 10^{15} fissions/s would be achieved with a 4 mA beam and a series of one-litre UnatC₃ targets, surrounding the Hg converter. Of all the fissions occurring in the UnatC₃ target, $\sim 90\%$ are induced by neutrons below 20 MeV. This is a positive fact since high-energy fissions produced by neutrons above 20 MeV tend to yield less neutron rich isotopes, as do those produced by protons, and present a more anisotropic distribution.

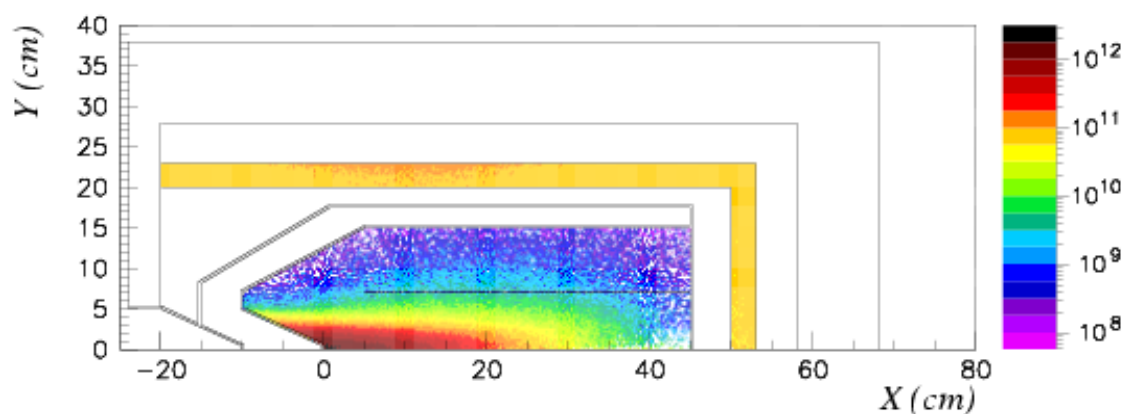


Figure 6. Fission density (fissions/ $\text{cm}^3/\text{s}/\text{MW}$ of beam) in the Hg converter and the UnatC₃ fission target.

Another key parameter in the design of the experiment is the power density, since it will determine the maximum beam intensity that the system can withstand, which in turn is correlated with the fission rate. As elaborated in [2], the energy deposition

peaks at ~ 2 cm downstream from the interaction point, rapidly decreasing radially (Figure 7.(a)).

The beam window is suffering smaller power densities (~ 900 W/cm³/MW of beam, Figure 7.(b)) due mainly to the lower density of stainless steel compared to Hg (7.8 vs. 13.5 g/cm³). This power density in the window requires a careful choice of material and cooling method, given that this is generally the weak point of liquid metal spallation targets.

The power density in the fission target seems rather homogeneous (~ 3 W/cm³/MW of beam) and follows, as could be expected, a spatial distribution similar to that of the fission density, consequently suggesting that this power is mostly originated by fission in U.

Detailed heat transfer calculations are necessary in order to study the final temperature distribution in the UCx and its impact on the ion extraction, although these power densities will not be high enough to heat up the fission target to the required ~ 2000 °C.

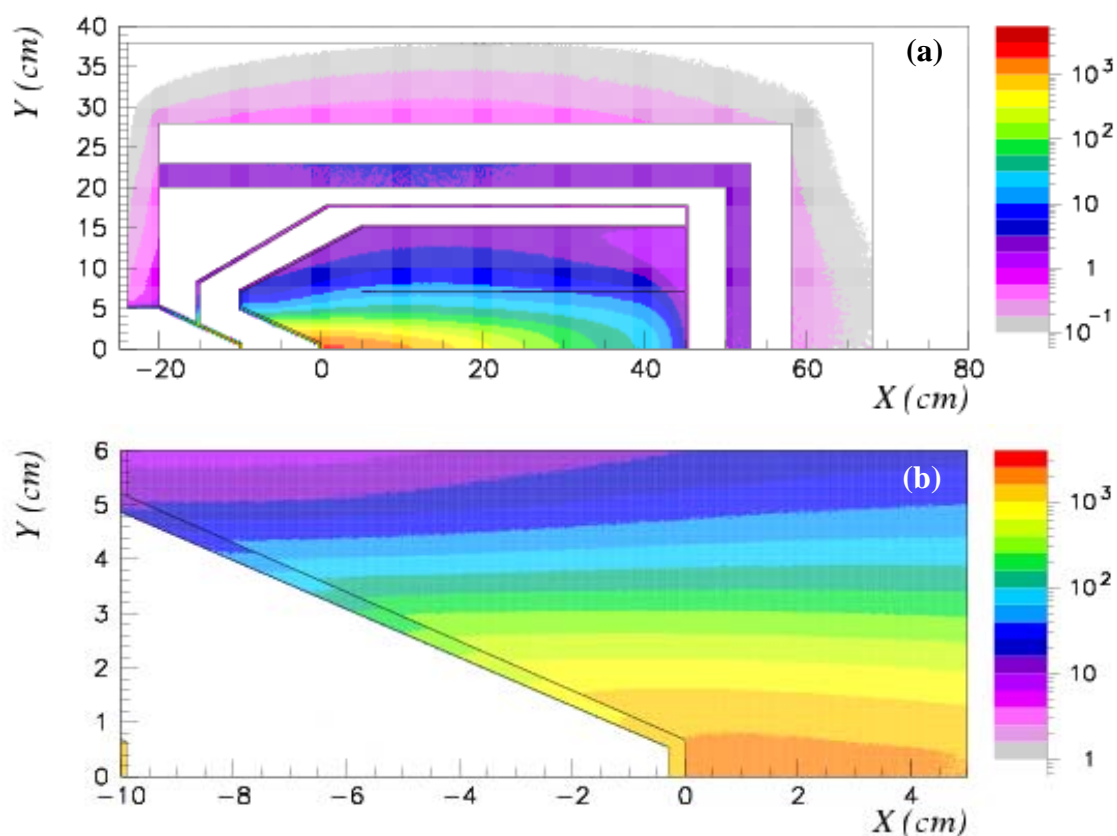


Figure 7. Power density distribution (W/cm³/MW of beam) in the Multi-MW target assembly (a), and close up around the Hg target window (b).

The power density in the target along the beam axis is shown in Figures 8.(a) and 7.(b), where the maximum power densities in the stainless steel container and the liquid Hg ($900 \text{ W/cm}^3/\text{MW}$ of beam and $1.9 \text{ kW/cm}^3/\text{MW}$ of beam, respectively) can be observed. A back-of-the-envelope calculation of the temperature increase in the Hg flow along the beam axis is also presented in Figure 8.(b), as a red curve. A Hg flow ($\rho=13.5 \text{ g/cm}^3$, $C_p=0.14 \text{ J/g/K}$) of 1 m/s and 5 MW of beam power were assumed. This curve shows that, although the boiling temperature is reached after 6 cm , the issue can be solved by increasing the flow rate, changing the design of the flow (e.g. transversal flow) or using a more homogeneously distributed beam shape (e.g. using a parabolic or wider beam, [2]). Finally, increasing the static pressure of the system to, for example, 5 bars would also considerably increase the Hg boiling temperature.

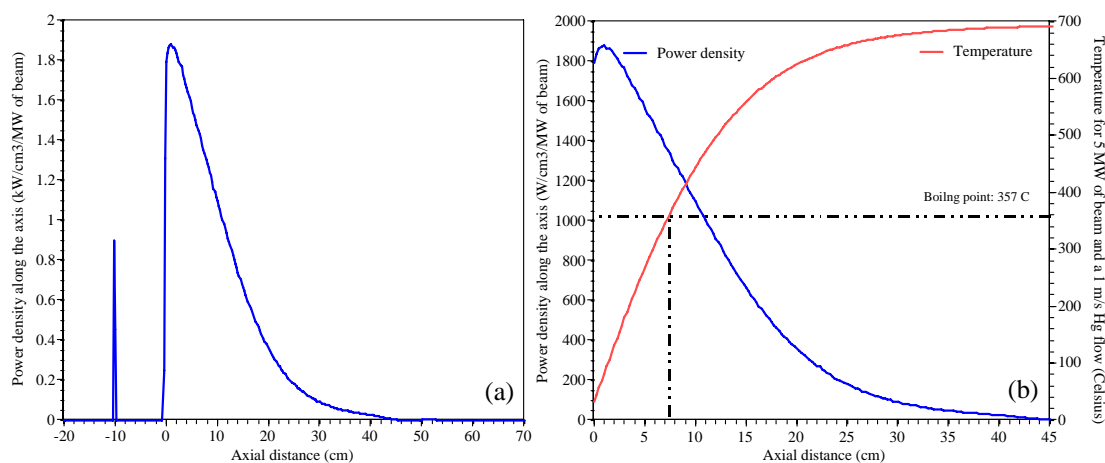


Figure 8. Power density distribution ($\text{kW/cm}^3/\text{MW}$ of beam) in the target assembly along the beam axis (a), and temperature increase for a 1 m/s flow and 5 MW (b).

High Density Fission Target

The high porosity required to enhance the diffusion and effusion processes in the fission target determines the relatively low density ($\rho \sim 3 \text{ g/cm}^3$) of the UC_3 fission targets. This low density somehow limits the number of fissions which can be achieved in a certain volume. Therefore, the possibility of using high-density ($\rho \sim 11 \text{ g/cm}^3$) fission targets, being studied by Task #4 of the EURISOL DS collaboration, seems an attractive one in order to obtain a maximum number of fissions in a reduced volume. Nevertheless, the use of these targets is subject to the ion extraction yield, which is the ultimate parameter to maximise.

Natural Uranium Carbide (UnatC)

One of the alternative fission targets studied was a 11 g/cm^3 uranium natural carbide, with a one-to-one ratio between U and C. This option would increase the fission density by a factor of 3 (to 3×10^{11} fissions/cm³/s/MW of beam), as shown in Figure 9, accordingly decreasing the current requirements to 1.7 mA to obtain 10^{15} fissions/s in a two-litre target. Equivalently and given that there is enough space around the Hg converter, one could place several fission targets to obtain a higher number of fissions. For instance, four 2.5-litre targets and 3.3 mA of beam current would produce $\sim 10^{16}$ fissions/s, one order of magnitude above the aimed value.

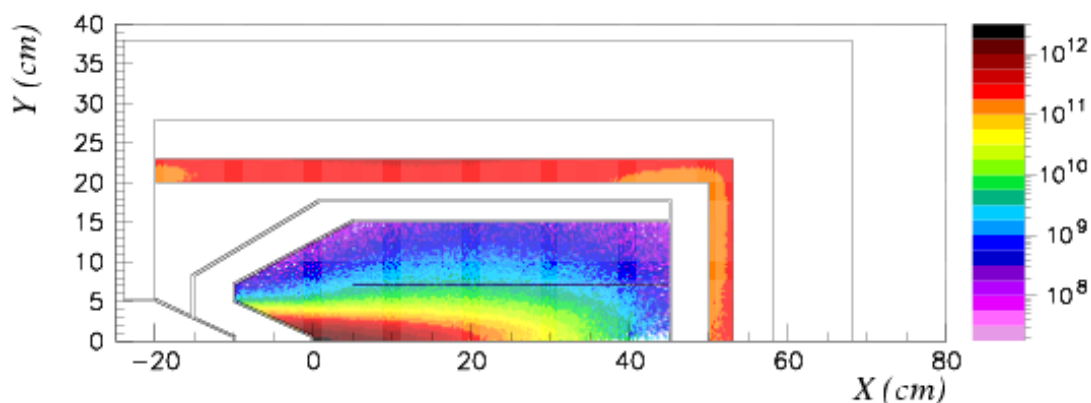


Figure 9. Fission density (fissions/cm³/s/MW of beam) for the baseline configuration and a high-density UnatC fission target.

The fission distribution is still very homogenous, as mentioned before, a very positive fact to enhance ion extraction. This increase in fissions also means a three-fold increase in power density to 10 W/cm^3 /s/MW of beam. Notice that these values are normalised to the same beam power, so if normalised to the number of fissions, power densities would be the same as in the case of low-density UnatC_3 .

On the other hand, the choice of a UnatC as fission target would have basically no impact on the neutron flux distribution (except for a small increase due to the larger number of fissions), neutron balance or on the ratio between fissions induced by neutrons above and below 20 MeV.

Depleted Uranium Carbide (^{238}UC)

The use of depleted uranium carbide fission targets was also contemplated. This option would avoid the use of a neutron reflector, since ^{238}U presents a fission threshold (around 600 keV). Therefore, a very marginal increase in number of fissions would be obtained thanks to a neutron reflector, while captures in ^{238}U would significantly increase and, consequently, also the production of Pu.

Figure 10 shows the fission density in this case ($\rho \sim 11 \text{ g/cm}^3$, ^{238}UC fission target and BeO reflector), where a rather anisotropic distribution may be observed. The average value of the fission density in the central part of the radial target (from 0 to 25 cm in length) is $\sim 1.3 \times 10^{11}$ fissions/cm³/s/MW of beam. This value is 2.3 times lower than the one obtained when natural U is used. Therefore, 60% of the fissions in the natural U target come from ^{235}U and 40% come from ^{238}U , for the same configuration (same fission target density and use of a neutron reflector).

The power density is also anisotropically distributed, peaking at $\sim 5 \text{ W/cm}^3$ /MW of beam. Therefore, in this case an alternative heating method would be necessary to obtain a homogeneous temperature in the fission target. As in the previous case, the primary particle and neutron flux distributions are not affected by the choice of fission target material.

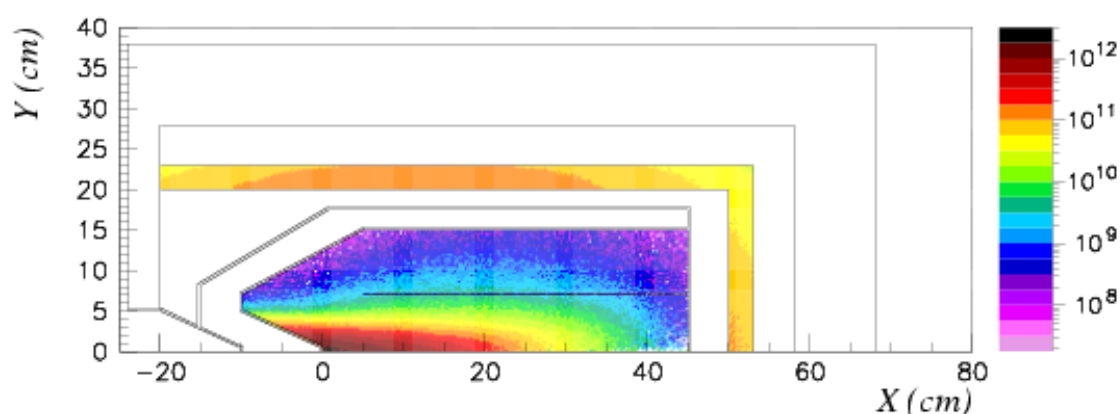


Figure 10. Fission density (fissions/cm³/s/MW of beam) for the baseline configuration and a high-density ^{238}UC fission target.

As previously mentioned, the 2.3 increase in fission rates when natural U targets are used is due to low-energy fissions in ^{235}U . This may be noticed, in Figure 11, by the

increase in the production rate of isotopes originated by asymmetric (low-energy) fissions. Some of the isotopes of interest for EURISOL lie in this region (e.g. ^{90}Kr and ^{134}Sn), hence an advantage of using natural U. A detailed analysis of specific isotopic yields is under progress.

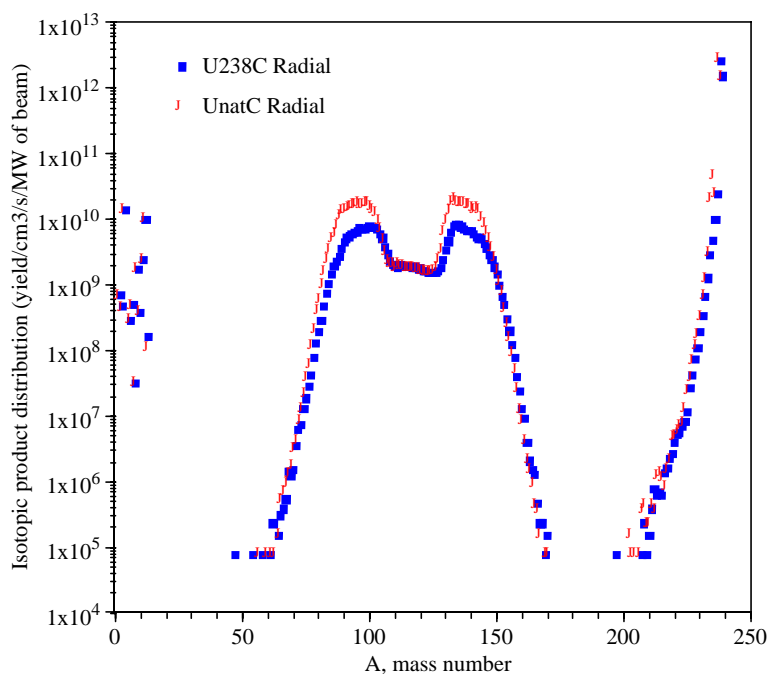


Figure 11. Isotopic yield distribution (yield/cm³/s/MW of beam) for two different fission targets.

These results, combined with the analysis carried out in [2], recommend the use of natural U in the fission target, since the fissions induced in ^{235}U are complementary to those induced in ^{238}U , and represent a 60% of the total when UnatC is used.

A detailed analysis of the fission target burn-up evolution is being performed to assess Pu concentrations and the build-up of radioactive inventory.

Use of a Neutron Reflector

The use of a neutron reflector around the fission target is an important option to study due to its possible impact on several essential design factors. Namely, the neutron economy, fission density and radioprotection would be positively affected by the backscattering of neutrons due to the reflector. A disadvantage may lie in the higher production of Pu, although this specific aspect needs to be studied in detail with an evolution code, given that Pu isotopes are generally very fissile at these energy range and inventories calculated with steady state methods will diverge from the real equilibrium concentrations.

In terms of particle confinement, the lack of reflector has some impact in the propagation of the few primaries escaping the Hg target ($\sim 10^9$ primaries/cm²/s/MW of beam), and particularly in the neutron escapes. The neutron flux outside the assembly increases by a factor of 2.

In the case of the low-density UnatC₃, the absence of reflector reduces the number of fissions in the uranium carbide to $\sim 2.9 \times 10^{10}$ fissions/cm³/s/MW of beam, that is 3.4 times fewer fissions than by using a 10 cm thick BeO reflector. For the UnatC high-density fission target the fission density is also significantly reduced by a factor of 2.1 (down to 1.4×10^{11} fissions/cm³/s/MW of beam). Moreover, the fission distribution becomes quite anisotropic, as shown by Figure 12, entailing possible mechanical problems due to temperature differences, mentioned in the previous section.

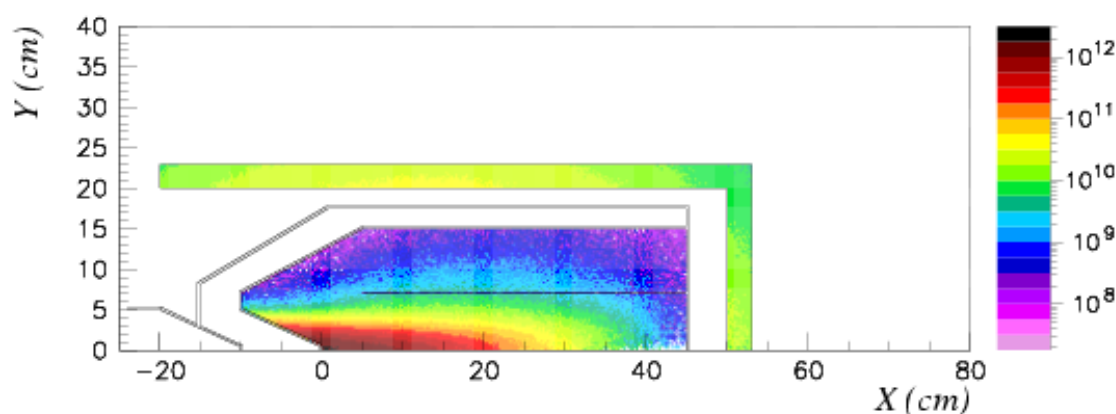


Figure 12. Fission density (fissions/cm³/s/MW of beam) in the Multi-MW UnatC₃ fission target without BeO reflector.

On the other hand, this design choice would not affect ²³⁸U fission targets (only $\sim 10\%$ reduction in fission density in both, high and low density, fission targets) since the majority of the neutrons are reflected back to the fission target at energies lower than those inducing fission in ²³⁸U. Namely, low-density ²³⁸UC₃ presents $\sim 3.1 \times 10^{10}$

fissions/cm³/s/MW of beam for a reflected layout and $\sim 2.7 \times 10^{10}$ fissions/cm³/s/MW of beam for an unreflected one.

Therefore, the use of a neutron reflector is highly recommended to increase the radioactive ion production in the fission target or equivalently reduce the requirements on the system to achieve a given fission rate (i.e. 10^{15} fissions/s). This is particularly true in the case of low-density natural uranium carbides, in which fissions rates are several times higher. Moreover, the use of BeO as reflector opens the possibility of producing ⁶He ions (n, α reactions on ⁹Be) required for β -beam applications.

2 GeV Proton Beam

The preliminary study of the liquid metal proton-to-neutron converter [2] showed that the use of a 2 GeV proton beam might be a positive choice to reduce 40% the maximum power density ($\sim 1.2 \text{ kW/cm}^3/\text{MW}$ of beam), thus alleviating the problems of heat removal, vaporisation and cavitation in the liquid Hg target. But this option would also have implications in parameters such as the primary escapes (the proton range in Hg increases by a factor of 2.5 at 2 GeV) or the fission yields (different neutron flux distribution and spectrum).

In the scope of this analysis, two target options were considered: a 85 cm long target meant to stop most of the primary shower; and also the possibility of keeping the target length to 45 cm, thus requiring a beam dump to stop the high-energy protons streaming beyond the target's end cap.

Extended Target Length

For a 2 GeV proton beam, extending the length of the Hg target to 85 cm would contain most of the primary proton shower ($\sim 10^{10}$ primary/cm²/s/MW of beam escaping the Hg with an average energy of 700 MeV, Figure 13), while keeping target dimensions reasonable.

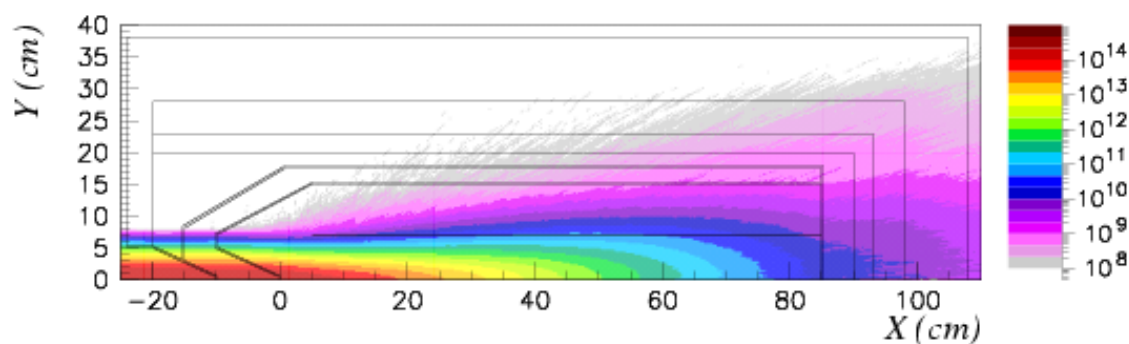


Figure 13. Primary proton flux (primary/cm²/s/MW of beam) for a 2 GeV proton beam and an extended Multi-MW target.

On the other hand, the neutron flux distribution would be modified, in particular in the end cap region, where the flux is strongly attenuated (Figure 14, $\sim 2 \times 10^{13}$ versus $\sim 10^{14}$ neutrons/cm²/s/MW of beam in the baseline configuration). This is due to the fact that most of the spallation neutrons are produced in the first 30 cm of the Hg target and the last section mainly moderates and absorbs low energy neutrons, scantily

contributing to the neutron production. Thus, the last 20 cm of the Hg converter mostly serve to contain the primary beam, even presenting a disadvantage in terms of neutron flux.

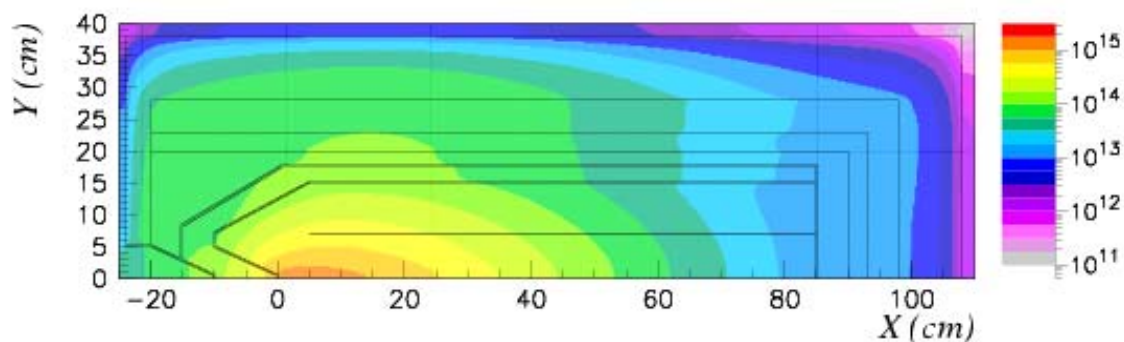


Figure 14. Neutron flux distribution (neutrons/cm²/s/MW of beam) for a 2 GeV proton beam and an extended target.

This is also reflected by the reduced fission density occurring in the end cap UnatC₃, one order of magnitude lower than the radial maximum. Moreover, this configuration produces a heterogeneous fission distribution, parallel to the decrease in neutron flux, as presented by Figure 15. For the sake of comparison, the average fission density in the region closest to the interaction point (from 0 to 25 cm in length, 20 to 23 cm radius) is $\sim 9.9 \times 10^{10}$ fissions/cm³/s/MW of beam, similar to the one in the baseline configuration, but anisotropically distributed.

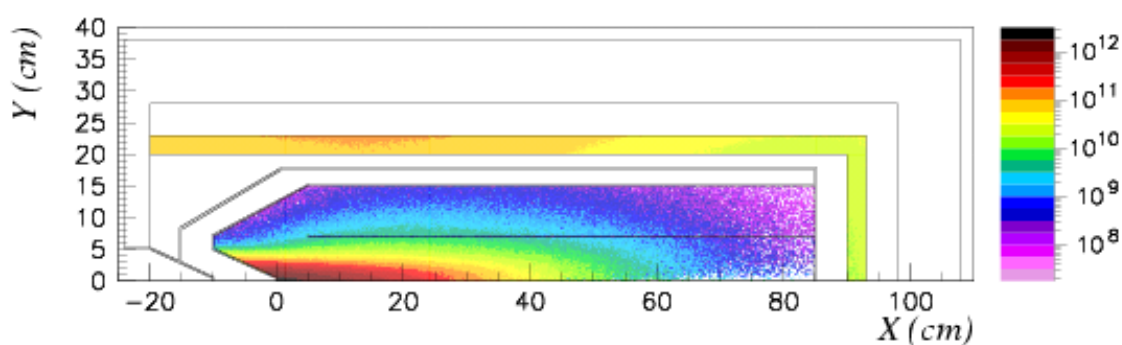


Figure 15. Fission density distribution (fissions/cm³/s/MW of beam) for a 2 GeV proton beam on an extended Multi-MW target assembly.

These results show that such a voluminous target may not be an optimal choice in terms of fission rates and technical feasibility. Thus the study of a 2 GeV proton beam on a shorter target may be of interest.

2 GeV Protons on a Short Target

The propagation of the proton primaries is rather forward-peaked, and the level of escapes through the end cap with this geometry is significantly higher, i.e. three orders of magnitude ($\sim 2 \times 10^{12}$ primary/cm²/s/MW of beam, Figure 16), compared to the use of 1 GeV protons. This fact would pose some problems in terms of radioprotection, since it would create a secondary neutron source outside the assembly, and damage the structures axially beyond the Hg target. Therefore, in such a design, a beam dump behind the Hg converter should be considered.

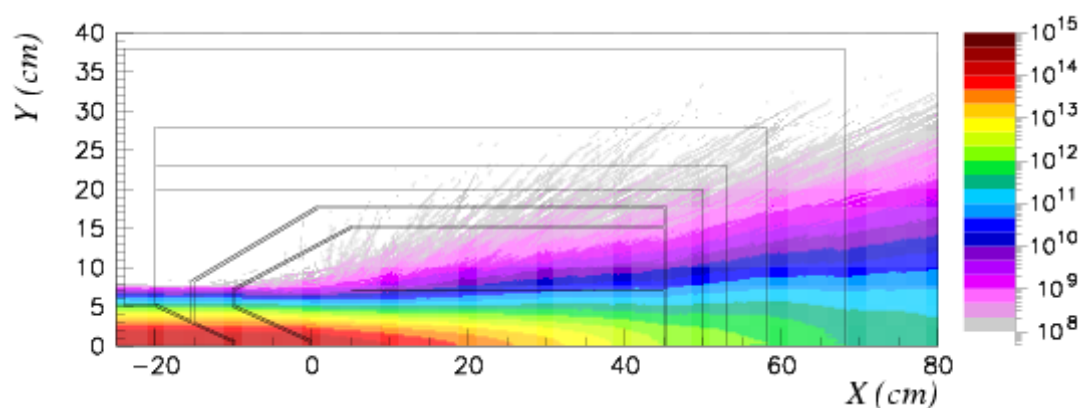


Figure 16. Primary proton flux (primary/cm²/s/MW of beam) for a 2 GeV proton beam on the baseline configuration.

The neutron flux distribution seems very similar to the one produced by a 1 GeV proton beam except for the flux increase in the end cap region (Figure 17), mostly due to very high-energy neutrons (above 100 MeV) travelling in the direction of the beam, and escaping the Hg after few interactions.

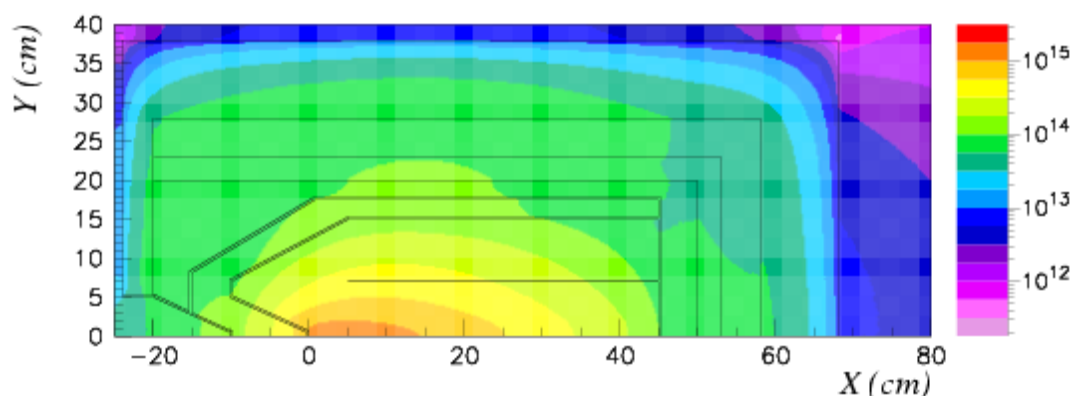


Figure 17. Neutron flux distribution (neutrons/cm²/s/MW of beam) for a 2 GeV proton beam on the baseline configuration.

The impact in the neutron spectrum can be perceived in Figure 18, where the energy distributions of neutrons exiting the radial and end cap surfaces are plotted. The resonances of Hg can be appreciated in both curves, together with a peak at ~ 300 keV, from evaporation neutrons which have been moderated, thus energy loss, inside the target. The most relevant difference lies in the high-energy range, since secondary neutrons emitted from direct nucleon-nucleon interactions tend to be more forward-peaked, as the proton energy increases. These high-energy neutrons may be problematic in terms of radioprotection given their potential biological hazard and damage to structural materials. Moreover, very high-energy (500 MeV to 1 GeV) neutrons escaping through the end cap will produce a new source of neutrons outside the target assembly.

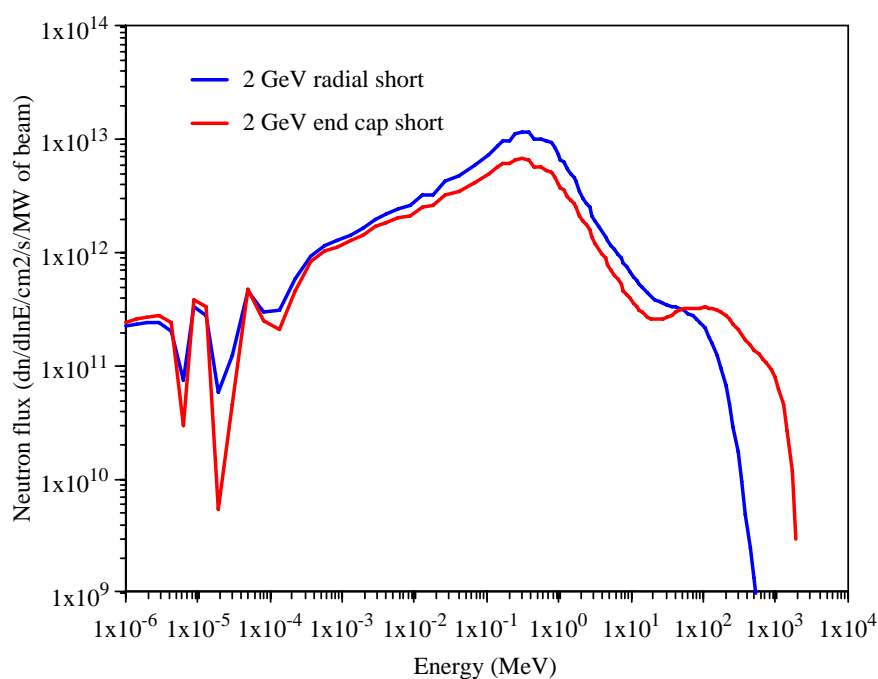


Figure 18. Comparison of the neutron flux energy distribution ($dn/dlnE/cm^2/s/MW$ of beam) for a 1 and 2 GeV primary proton beam.

In terms of fission densities, there is no difference between the use of a 1 GeV or a 2 GeV with the baseline configuration (values of $\sim 10^{11}$ fissions/cm³/s/MW of beam, in both cases), except for a slightly higher fission density in the target placed behind the end cap.

To have a first estimate of the activation and isotope production inside the Hg, residual nuclei yields in the converter were evaluated. Figure 19 shows the mass distribution of the elements produced by the proton beam on the Hg isotopes, for 1 and 2 GeV primaries (normalised to 1 MW of beam power). The largest differences occur in the regions between A 10 – 60 and 140 – 160. These are elements produced

by multi-fragmentation on Hg, reaction channel competing with evaporation and gaining weight with increasing energy. The distribution of both curves suggests that a 2 GeV beam may produce more spallation products in the liquid metal; a detailed analysis of the time evolution of the activity caused by specific isotopes should be performed.

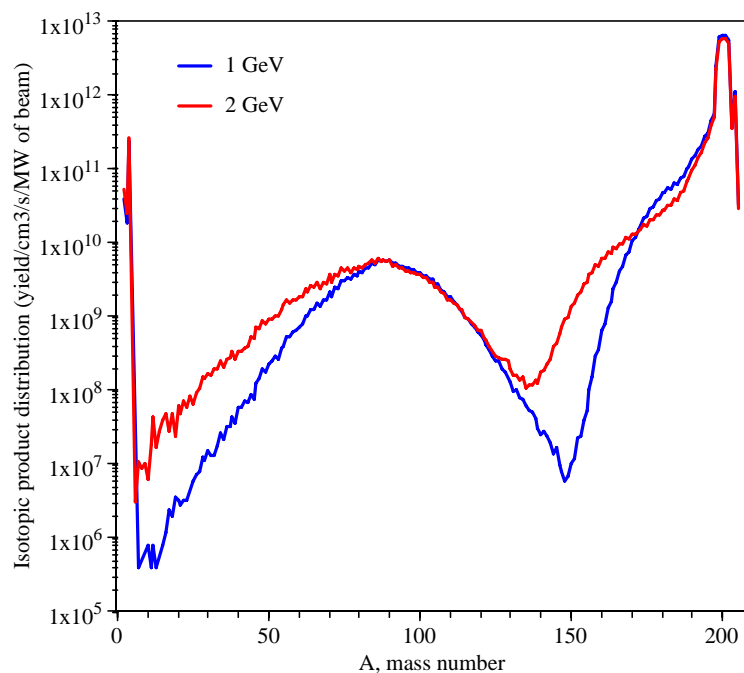


Figure 19. Residual nuclei distribution (isotopes/cm³/s/MW of beam) in the liquid Hg for different proton beam energies.

Integration of the Assembly

These calculations were performed using a simplified geometry of the assembly. In order to integrate all the components, new elements (e.g. mechanical, electrical...) shall be required.

The cylindrical Hg target presents a conical beam window to enhance the heat distribution and to reduce the backscattering of secondary particles. The whole Hg target is confined inside a stainless steel hull, to avoid Hg spillage in case of a leak from the primary container, and to allow the cooling of the beam window by using a He gas flow. Inside the Hg target, the liquid metal flow is guided by an inner tube in order to separate the incoming and outgoing flow. This tube may present some openings to avoid no-flow regions.

The Hg cooling circuit may be similar to that used in SNS and designed for ESS. In fact, the use of Hg as liquid metal presents important advantages for radioprotection

in the cooling circuit, given the reduced production of α -emitters, as opposed to the use of Lead-Bismuth Eutectic (Po production).

The Hg target unit should be integrated inside a stainless less vacuum chamber, which would also contain the fission targets and ion-extraction lines. The whole assembly should be is shielded by a neutron reflector, which also increases the neutron economy. The experimental hall will have to be surrounded by several meters of concrete to stop any secondaries (i.e. neutrons, photons and muons) from spacing the facility and inducing radiation doses outside the area assigned to the experiment.

The fission target should be thermally and electrically insulated from the Hg converter, to avoid heating up the later, as well as to allow the electrical grounding of the converter while the fission target is set to ~ 60 kV for the ion extraction. The connectors to apply this voltage should be place on both ends of the target, with the ion extraction channels placed in the middle.

The Hg converter should be as compact as possible to keep the dimensions of the assembly reasonable, avoiding structural complexity due to weight and allowing setting the system in a horizontal position.

The design of a beam stop should be contemplated, in particular if 2 GeV protons are chosen and the converter length is kept the same.

Conclusions

These simulations show the technical feasibility of such a Multi-MW target design and the possibility to achieve the aimed fission rates with a reduced fission target volume. The neutronic parameters of a baseline configuration were characterised and several design options assessed.

This baseline configuration successfully contains most of the primary beam, producing a rather isotropic and intense ($\sim 10^{14}$ neutrons/cm²/s/MW of beam) neutron flux, which yields an important and homogeneous fission rate in the uranium carbide target.

Power densities are still an issue, particularly in the beam window (~ 900 W/cm³/MW of beam) for which an adequate material should be foreseen and the cooling method optimised. As elaborated in [2], a parabolic beam profile would also improve the power densities by factor of 2, bringing down the maximum to ~ 1 kW/cm³/s/MW of beam. This fact, combined with an optimum design of the Hg flow, may successfully evacuate the energy deposited the converter, avoiding boiling and cavitation problems.

For the fission target, it has been shown that the use of natural U combined with a neutron reflector increases at least by a factor of 2 the number of fissions. A series of one-litre UnatC₃ targets (such as the ones used in ISOLDE) and 4 mA of beam current are capable of producing the aimed 10¹⁵ fissions/s. If high-density UC targets were used, the rates are increased by a factor of 3, bringing about isotopic yields higher than expected and alleviating the beam requirements on the proton-to-neutron converter.

Finally, the use of a 2 GeV proton beam may reduce the power densities, but at the expense of either a more voluminous target, or high-energy particle escapes along the beam line and envisage a beam dump. At higher proton energies, the neutron yields are not increasing, since the beam current is proportionally reduced to normalise to the same beam power, and neither are fission rates.

Acknowledgements

We acknowledge the financial support of the European Commission under the 6th Framework Programme “Research Infrastructure Action- Structuring the European Research Area” EURISOL DS Project Contract no. 515768 RIDS. The EC is not liable for any use that may be made of the information contained herein.

References

- [1] “EURISOL DS; European Isotope Separation On-Line Radioactive Ion Beam Facility Design Study”, EC – FP6 Research Infrastructure Action- Structuring the European Research Area, Project Contract no. 515768 RIDS.
- [2] A. Herrera-Matínez, Y. Kadi, “Preliminary Study of the Liquid Metal Proton-to-Neutron Converter”, EURISOL DS/TASK2/TN-05-01 and CERN-AB-06-013 ATB.
- [3] A. Fassò, A. Ferrari, J. Ranft, P.R. Sala, “FLUKA: Status and Prospective for Hadronic Applications”, invited talk in the Proceedings of the MonteCarlo 2000 Conference, Lisbon, October 23--26 2000, A. Kling, F. Barao, M. Nakagawa, L. Tavora, P. Vaz eds., Springer-Verlag Berlin, p. 955-960, 2001. Also: “Electron-photon transport in FLUKA: Status”, A. Fassò, A. Ferrari, P.R. Sala, invited talk in the Proceedings of the MonteCarlo 2000 Conference, Lisbon, October 23--26 2000, A. Kling, F. Barao, M. Nakagawa, L. Tavora, P. Vaz eds., Springer-Verlag Berlin, p. 159-164, 2001.

- [4] J. Cornell (Ed.), “*The EURISOL Report; A Feasibility Study for a European Isotope-Separation-On-Line Radioactive Ion Beam Facility*”, GANIL, France, 2003.